Available online at www.sciencedirect.com
ScienceDirect
International Journal of Heat and Mass Transfer 50 (2007) 4527–4539
International Journal of HEAT and MASS TRANSFER
www.elsevier.com/locate/ijhmt

An experimental data set for benchmarking 1-D, transient heat and moisture transfer models of hygroscopic building materials. Part I: Experimental facility and material property data

Prabal Talukdar [a], Stephen O. Olutmayin [b], Olalekan F. Osanyintola [c], Carey J. Simonson [b,*]

[a] Department of Mechanical Engineering, Indian Institute of Technology Delhi, Hauz Khas, New Delhi 110 016, India
[b] Department of Mechanical Engineering, University of Saskatchewan, 57 Campus Drive, Saskatoon, SK, Canada S7N 5A9
[c] XXL Engineering Ltd., #101-807 Manning Road NE, Calgary, AB, Canada T2E 7M8

Received 31 March 2006; received in revised form 17 March 2007
Available online 7 June 2007

Abstract

As numerical models of heat and moisture transfer in porous building materials advance and numerical investigations increase in the literature, there remains a need for simple accurate and well-documented experimental data for model validation. The aim of this two part paper is to provide such experimental data for two hygroscopic building materials (cellulose insulation and spruce plywood) exposed to 1-D and transient boundary conditions. Part I of this paper describes the transient moisture transfer (TMT) facility used to generate the experimental data as well as the uncertainty and repeatability of the measured data. The measured material properties are also presented to fully document the experimental data set and permit its use by other researchers.

Keywords: Heat and moisture transfer; Porous building materials; Experiment; Sorption isotherm; Water vapour permeability; Hygroscopic materials

1. Introduction

Modern buildings and their heating, ventilating and air-conditioning (HVAC) systems are required to be more energy efficient, while considering the ever-increasing demand for better indoor air quality, performance and environmental issues. The goal of HVAC design in buildings is to provide good comfort and air quality for occupants during a wide range of outdoor conditions. There is a lot of research aimed at improving the HVAC systems in buildings while reducing the energy costs and environmental impacts. Some studies relate to control strategies and protocols [1–3] while others focus on the analyses of specific components such as heat pumps [4,5], photo voltaic cells [6] and evaporative cooling towers [7] to name a few. In order for these systems to have the greatest impact, it is important for the energy needs of the building to be reduced as much as practical. One way to do this is to reduce the heat losses and gains through the building envelope by selecting proper insulating materials which are often porous and hygroscopic.

In addition to reducing heat losses and gains, research [8–13] has shown that hygroscopic building materials can moderate relative humidity variations, affecting the perceived air quality [14] and energy consumption [15]. This is important because recent research by Fang et al. [16] and Toftum and Fanger [17] has shown that outdoor ventilation rates could be decreased if a moderate enthalpy is maintained in spaces (provided the minimum ventilation for health is satisfied) [17].

Over the past half century, a lot of research has been done on heat, air and moisture (HAM) transfer and storage in building materials and their effect on energy consumption and the durability of the building. Several large, international projects have been completed in this field in the

* Corresponding author. Tel.: +1 306 966 5479; fax: +1 306 966 5427.
E-mail address: carey.simonson@usask.ca (C.J. Simonson).

0017-9310/$ - see front matter © 2007 Elsevier Ltd. All rights reserved.
doi:10.1016/j.ijheatmasstransfer.2007.03.026

Nomenclature

A	exposed area of test section (m^2)
C_p	specific heat capacity at constant pressure (J/(kg K))
C_d	orifice discharge coefficient
d	diameter across the orifice plate (m)
D	diameter of the supply duct (m)
D_a	binary diffusion coefficient for water vapor in air (m^2/s)
D_{eff}	effective vapour diffusion coefficient (m^2/s)
D_h	hydraulic diameter of the test section duct (m)
h_a	convective heat transfer coefficient (W/(m^2 K))
h_{ad}	latent heat of adsorption (J/kg)
h_{fg}	latent heat of vapourization/sorption (J/kg)
h_m	convective mass transfer coefficient (m/s)
k_{eff}	effective thermal conductivity (W/(m K))
m	mass of specimen (kg)
m_o	mass of dry specimen (kg)
$\dot{m}$	rate of phase change (kg/(m^2 s))
$\dot{m}_a$	mass flow rate of air (kg/s)
Nu	Nusselt number
P_{atm}	atmospheric pressure (N/m^2)
P_{vsat}	saturation vapour pressure (N/m^2)
q''	heat flux (W/m^2)
R_v	specific gas constant of vapour (J/kg K)
Re	Reynolds number of airflow over the specimen
RH	relative humidity
S	sensitivity coefficient for the material properties
Sh	Sherwood number
t	time (s) or (h) if specified
T	temperature (°C)
TMT	transient moisture transfer
u	mass of moisture adsorbed per kg of dry specimen (kg/kg)
W	humidity ratio (kg/kg)
x	distance from the top of the specimen (m)

Greek symbols

β	diameter ratio
δ	water vapour permeability (kg/(m s Pa))
Δm	moisture accumulation (kg)
Δp	pressure difference (Pa)
ΔT	temperature difference (K)
ε	volume fraction
λ	expansibility factor
ρ	density (kg/m^3)
ϕ	relative humidity in fraction

Subscripts

a	air
atm	atmospheric
av	average
eff	effective
g	gas phase (air and water vapour)
i	initial, at some point
j	index
l	adsorbed phase
s	solid
v	vapour
vsat	saturation vapour

last decade [18–21] as well as numerous studies by individual researchers and organizations, e.g., [22–25]. These studies have significantly advanced this field of research, but have also highlighted the general need for more experimental data that quantifies HAM transport in porous building materials. For example, Hagentoft et al. [19] provide excellent benchmarks for assessing the quality of 1-D HAM simulation models, but rely solely on numerical and analytical cases because well-documented and accurate 1-D data are scarce. Therefore, the main purpose of this paper is to present a detailed description of a test facility that provides data that quantifies transient, 1-D heat and moisture transfer in building materials, including the accuracy, repeatability and the extent to which the experiments are 1-D. These are important factors when using the data in part II of the paper [26], to validate numerical models.

In the current research, two porous and hygroscopic building materials are chosen for investigation – cellulose insulation and spruce plywood. Since the experimental results in part II [26] are intended as a data set to benchmark numerical simulations, the material properties like sorption isotherm, thermal conductivity and water vapour permeability are also required to fully document the data set. These properties are input parameters for numerical models and may significantly affect the numerical results and therefore the experimental procedures and measured property data are presented in this paper.

2. Experimental facility

The purpose of the experiment is to measure the transient temperature, relative humidity and moisture accumulation distributions within cellulose insulation and spruce plywood.

2.1. Facility

A schematic of the transient moisture transfer (TMT) facility is shown in Fig. 1. The facility is designed to measure 1-D heat and moisture transfer between a flowing air stream and a stationary porous material. A small converging wind tunnel produces a steady, fully developed air flow above the material to be tested. The airflow is provided by a variable speed vacuum pump, which draws air from one

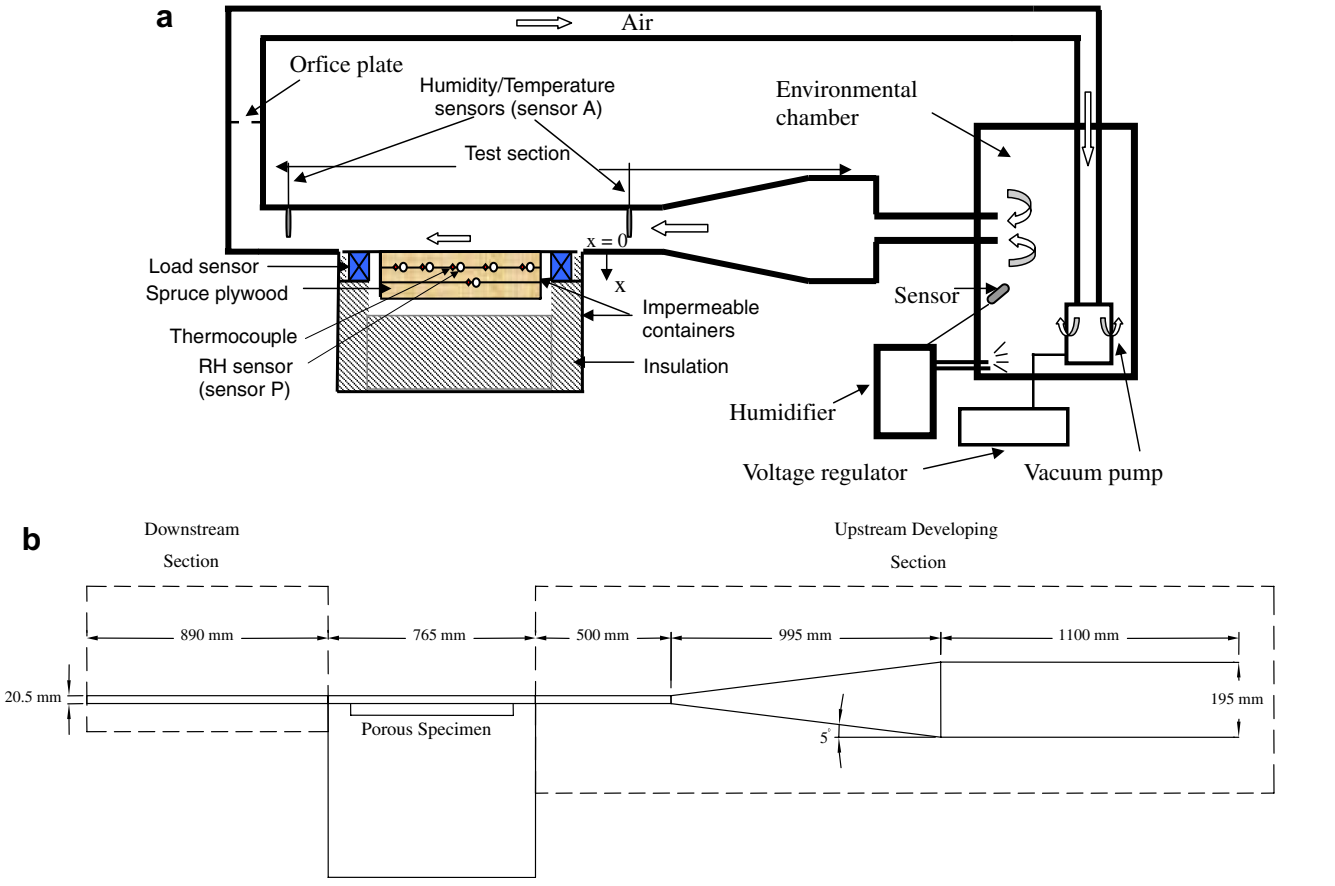

Fig. 1. Schematic of (a) the TMT facility and (b) test section.

of two environmental chambers that can be maintained at different temperatures and humidity. Transient test conditions are created by switching the chamber from which the air is delivered. Fig. 2 presents the temperature and humidity in the environmental chamber during a 2-day test showing the typical fluctuations during a test. In Fig. 2, 95% of the data are within ±0.1 °C and ±1.4% RH of the average. The closed loop ducting system helps minimize fluctuation in air temperature and relative humidity.

The airflow in the rectangular duct (20.5 mm high and 298 mm wide) above the test section (Fig. 1b) creates the upper convective heat and moisture transfer boundary condition for the material being tested, while a plate heat exchanger and insulation creates the lower boundary condition. The plate heat exchanger can be controlled to a specified temperature or left inactive (as in this paper) resulting in an adiabatic boundary condition below the test specimen. The test material is contained in a container made of lexan plastic which creates an impermeable boundary condition on the bottom and all sides of the specimen. The impermeable plastic container ensures 1-D moisture transport, while the insulation around the container creates an adiabatic boundary condition resulting in 1-D heat transfer. The size of the plastic container depends on the thermal and moisture properties such as density, porosity, thermal conductivity and water vapour

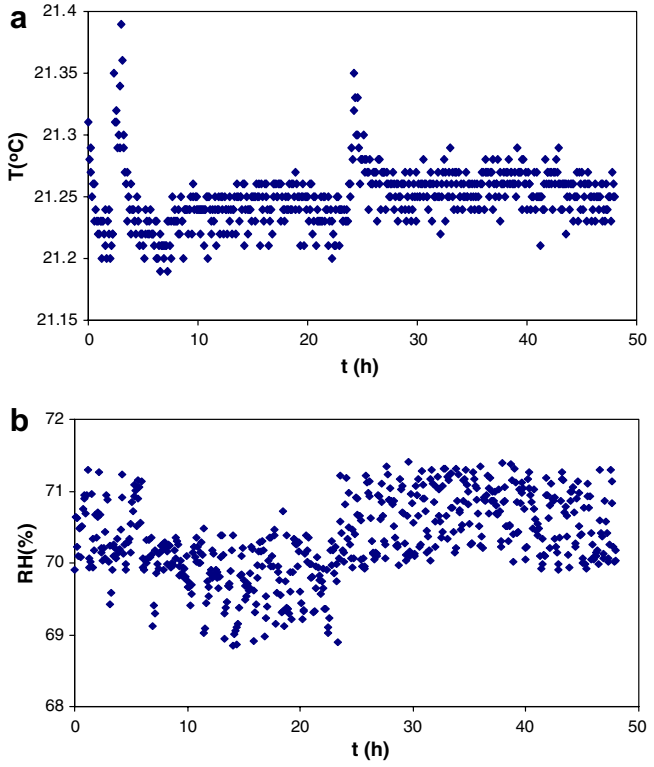

Fig. 2. Measured (a) temperature and (b) relative humidity of air in the environmental chamber shown for a period of 2 days.

permeability of the material to be tested. For the experiments in this paper, the container is chosen to be 600 mm long, 280 mm wide, 27 mm deep for spruce plywood and 600 mm long, 280 mm wide, 300 mm deep for cellulose insulation. For the measurements of spruce plywood, three pieces of plywood (each 9 mm thick) are held together with nylon screws to reduce the air gap between the pieces (Fig. 3). In the case of cellulose insulation, cellulose is packed to a uniform density of 50 kg/m^3 inside the container.

In addition to well defined boundary conditions, a complete data set requires specified initial conditions. The initial conditions were achieved by conditioning the spruce plywood boards until they are in equilibrium with air above a saturated salt solution ($KC_2H_3O_2$–22% RH), with equilibrium being defined as when the change in mass between three successive readings 24 h apart is less than 0.1%. The cellulose insulation is conditioned to equilibrium with the laboratory air because it is a loose fill material and difficult to remove from the container.

3. Instrumentation and uncertainty

The full data set includes many measurements of temperature, relative humidity, mass and pressure drop. These data are measured with sensors throughout the TMT facility and recorded using 16-bit and 12-bit analogue to digital acquisition cards. To ensure high precision, the 16-bit card is used to record the temperature from the T-type thermocouples and the moisture accumulation from the gravimetric load sensors. The 12-bit card is used record the relative humidity from the humidity sensors, temperature from the RTD sensors and pressure difference from the pressure differential gauge. All the sensors used in the TMT facility (i.e., relative humidity sensors, gravimetric load sensors and thermocouples) are calibrated with known standards before and after the tests. All the sensors used in the experiments show good agreement between the pre-test and post-test calibrations and the total uncertainties (root sum square of bias and precision uncertainties) are summarized in Table 1. The calibration of each sensor and the

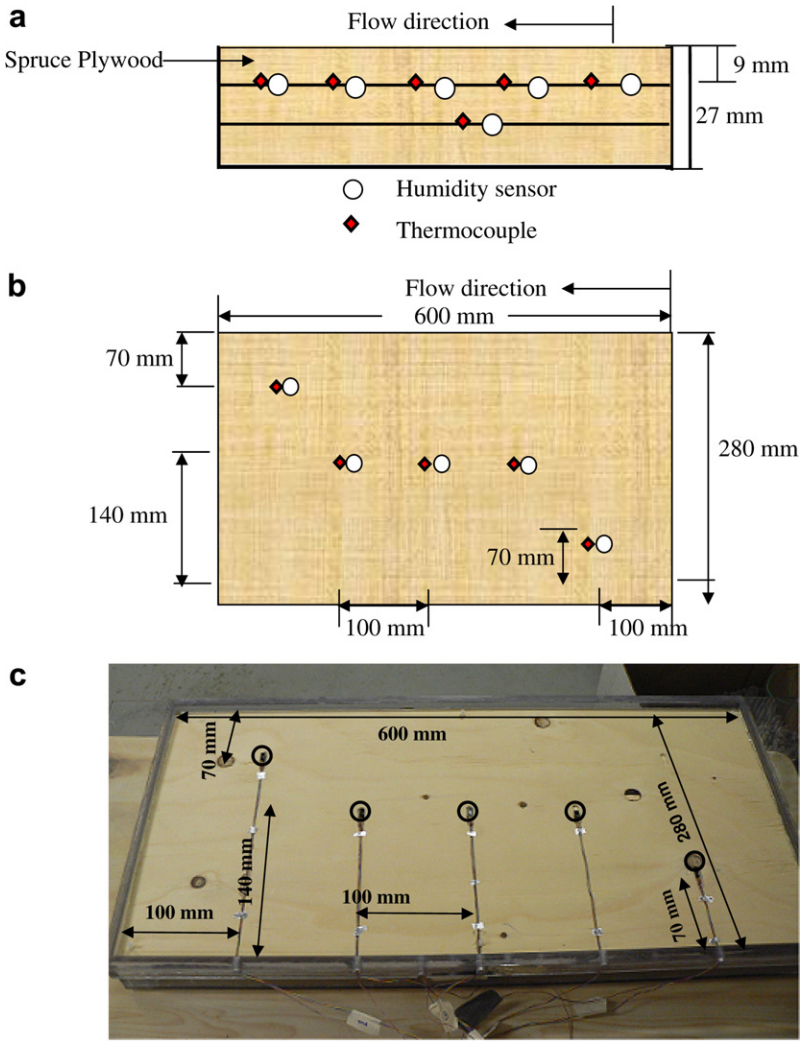

Fig. 3. Location of the thermocouple and humidity sensors between the layers of spruce plywood: (a) side view, (b) top view at a depth of 9 mm and (c) top view picture showing the grooves in the plywood.

Table 1
Uncertainties in the different sensors used in the experiment

Sensor name used in the text	Location	Description	Total uncertainty
Temperature			±0.1 °C
Humidity sensor A	Used in air stream	Largest sensor with a perforated cylinder shield (61 mm long × 12.6 mm in diameter)	±1.1%
Humidity sensor C	Used in the cellulose bed	Smaller sensor with a small cubic shield (20 mm × 9.8 mm × 4.8 mm) to reduce influence in the bed. The shield is needed to protect the sensor from contact with the cellulose fibers	±1.2%
Humidity sensor P	Used in the plywood bed	Smallest sensor (9.4 mm × 4.2 mm × 2 mm) with no shield required because it is placed in the grooves between the plywood boards	±1.3%
Mass accumulation	With load sensor With RH sensor		±2 g (±2%) ±15%
Mass flow rate Reynolds number			±6% ±8%

location of the sensors in the TMT are presented in the following sections.

3.1. Temperature measurements and calibration

The temperature of air entering and leaving the test section is measured with RTD sensors that are part of the humidity/temperature transmitter (sensor A). All other temperatures are measured using T-type thermocouples. The temperature sensors are calibrated using a temperature simulator that has a bias uncertainty of 0.1 °C as a transfer standard. The calibration is performed over a large temperature range (−40 °C to 40 °C) and the average difference between the readings from the sensors and the simulator is less than 0.1 °C. For the temperature range studied in this paper (20–30 °C), the differences are less than 0.05 °C. The bias uncertainty of the temperature sensors are therefore ±0.1 °C.

For the temperature distribution measurements within the spruce plywood, six thermocouples are arranged between the individual pieces of spruce plywood as shown in Fig. 3. The sensors are positioned in small grooves (2 mm wide by 0.5 mm deep) machined in each pieces of plywood and the sensor leads are in grooves (6 mm wide by 0.5 mm deep) (Fig. 3c). These grooves allow the plywood boards to maintain contact when the bed of plywood is compressed with the plastic screws. Five thermocouples are placed at a depth of 9 mm, equally spaced horizontally in the flow direction (100 mm apart) and across the flow direction (70 mm apart) as shown in Fig. 3. A single thermocouple is placed at a depth of 18 mm. These sensors measure the 3-D temperature field within the spruce plywood and will be used in Section 4 to verify that the temperature field is essentially 1-D.

For cellulose insulation, 26 thermocouples are arranged in the cellulose insulation bed as shown in Fig. 4. The thermocouples are placed at vertical increments of 30 mm. Five thermocouples are placed at a depth of 150 mm and 300 mm and are equally spaced horizontally as shown in Fig. 4b. Two thermocouples are placed at all other depths as shown in Fig. 4a.

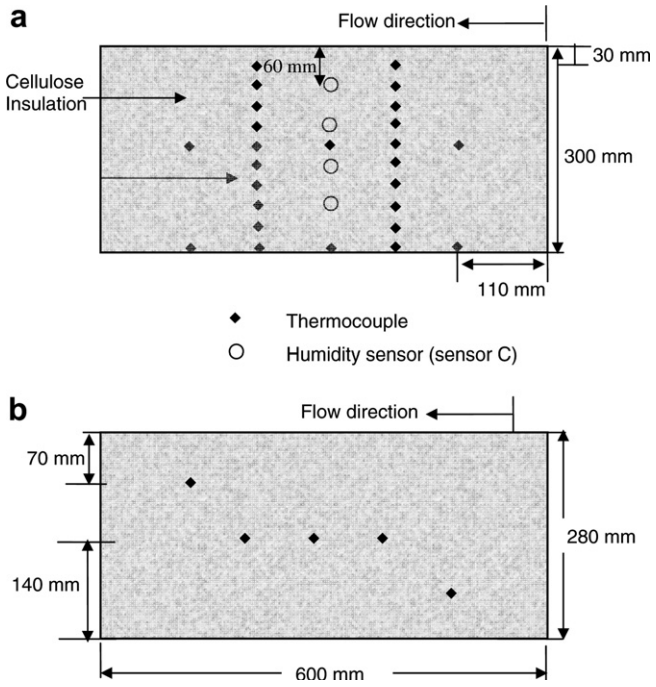

Fig. 4. Side view (a) and top view at a depth of 150 mm (b) of the temperature and humidity sensor arrangement within the cellulose insulation bed.

3.2. Relative humidity measurement and calibration

The relative humidity is measured for air entering and leaving the test section (Fig. 1a) as well as within the hygroscopic material to be tested (Figs. 3 and 4). Different sensors are used in the different positions and materials and these are chosen to minimize uncertainty, while reducing sensor size in the porous material. The relative humidity of air entering and leaving the test section is measured with the same instrument used to measure the inlet and outlet air temperature.

The sensor is labelled sensor A because it measures the humidity in the air stream. For the measurements of relative humidity within the spruce plywood, small capacitance type humidity sensors made by Honeywell (labelled sensor P for plywood) are embedded between the layers of the spruce plywood. The humidity sensors are at the same location as the thermocouples. For the case of the cellulose insulation bed, four sensors manufactured by TDK (labelled sensor C for cellulose) are used to measure the relative humidity within the bed. They are placed at the same locations as the thermocouples. These locations are 0.06 m, 0.12 m, 0.18 m and 0.24 m from the top surface. There is only one measurement of the relative humidity at each location, and these measurements are at the centre of the bed. Descriptions of all the sensors used in the experiments along with their uncertainties are summarized in Table 1.

The humidity sensors relate the electrical capacitance of the sensor material, which changes with air relative humidity, to the relative humidity of the surrounding air. As these are very sensitive to contamination and drift over time they must be calibrated very rigorously. A chilled mirror with a bias uncertainty of ±0.5% RH is the transfer standard for calibrating all the humidity sensors. The humidity sensors are calibrated in air starting at a relative humidity of 10% with an increment of 10% RH up to 90% RH. With these measurements, a calibration equation is developed for each sensor to correct the RH readings and the difference between the corrected sensor readings and the chilled mirror reading are presented in Fig. 5a and b. The maximum difference between corrected sensor RH and chilled mirror RH is ±0.8% for sensor A (air) and ±1% RH for sensors P (plywood) and C (cellulose). Including the ±0.5% RH bias of the chilled mirror sensor, the total bias uncertainties in the sensors are ±0.9% for sensor A and ±1.1% for sensors C and P. A second calibration test is performed in air to check the repeatability of the sensors. These data show that the precision uncertainty of the sensor is ±0.6% for sensors A and C, and ±0.7% for sensor P, giving a total uncertainty (root-sum square of the bias and the precision) of ±1.1% RH, ±1.2% RH and ±1.3% RH for the sensors used in the air stream (sensor A), cellulose bed (sensor C) and the plywood bed (sensor P) (Table 1).

The humidity sensors used in the cellulose bed may be affected by being packed in the bed of cellulose insulation. To investigate this, these sensors are packed in cellulose and recalibrated at 30%, 50%, 70% and 90% RH. The differences between the RH readings during the calibration in air and cellulose insulation are shown in Fig. 5c. The maximum difference between the calibration in air and cellulose insulation is 0.8% RH, with 95% of the data within ±0.5% RH. These differences are comparable to the precision uncertainty of the sensors, and slightly less than the bias uncertainty, which means that the humidity sensors can be used to accurately measure the relative humidity when packed in the bed of cellulose insulation. No additional uncertainty is needed to account for the fact that sensor C is packed within the cellulose bed.

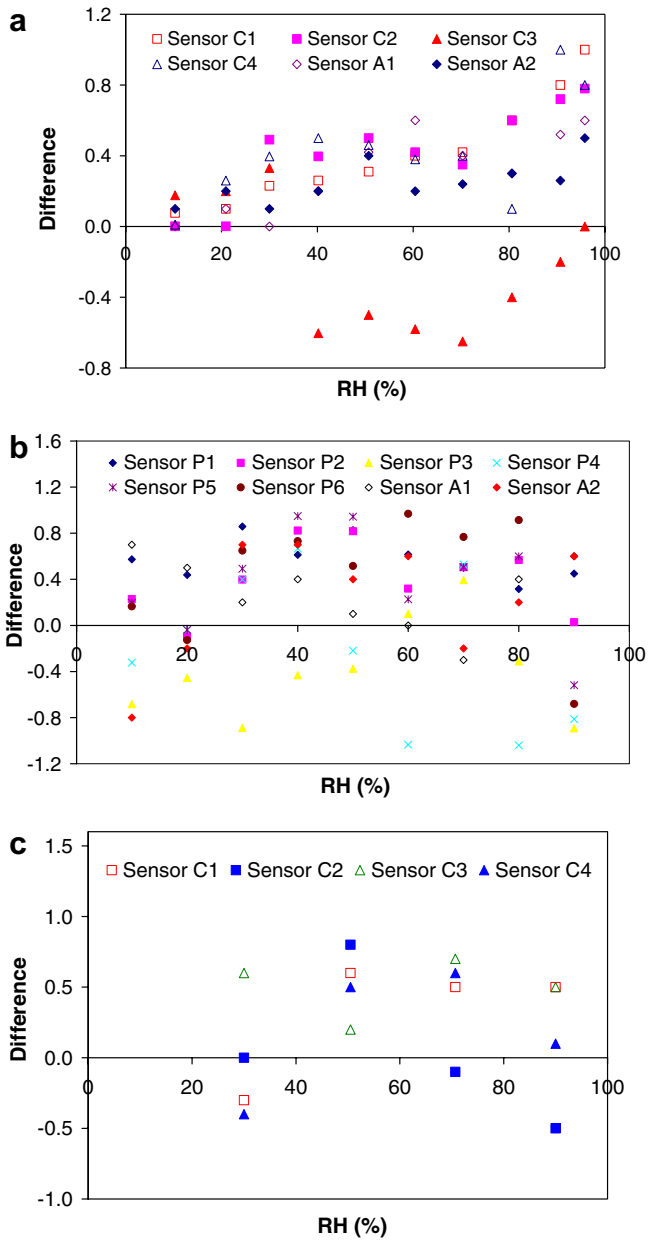

Fig. 5. The difference between the corrected sensor reading and chilled mirror reading for the calibration of the relative humidity sensors in air for (a) cellulose, (b) plywood and (c) the difference between the readings of humidity sensors in air and cellulose insulation at different calibration points.

3.3. Moisture accumulation measurement and calibration

The main sensors used to measure the change in mass of the material being tested due to adsorption and desorption of moisture are compression type, gravimetric load sensors. The plastic container in the test section is free floating on four gravimetric load sensors and thus any change in mass during the experiment is the mass of moisture adsorbed into or desorbed from the porous bed. The load sensors are calibrated in situ by placing the plastic container with the porous material inside the test section and adding

calibration masses. Calibration masses in the range of 1–500 g with a bias uncertainty of ±0.1 g are used to calibrate the load sensors. The calibration shows that the load sensors have a very high sensitivity and respond to changes in mass as small as 1 g. The maximum difference between the calibration weights and the load sensor readings is 2 g which equates to about ±2% at the end of a test. To increase confidence in the experimental data, the change in moisture content is determined using the temperature and humidity sensors in the air stream at the entrance and exit of the test section and the measured mass flow rate of air above the porous material (Section 3.4). Integrating with time the difference between the humidity ratio of the air entering and leaving the test section and multiplying by the mass flow rate gives

$$\Delta m(t) = \int_0^t \dot{m}_a (W_{inlet} - W_{outlet}) dt, \quad (1)$$

where Δm is the moisture accumulated in the bed (positive for moisture accumulation and negative for moisture removal), $\dot{m}_a$ is the mass flow rate of the air, W_{inlet} and W_{outlet} are the humidity ratios of the air entering and leaving the test section, respectively,

$$W = \frac{0.62198\,\phi P_{vsat}}{P_{atm} - \phi P_{vsat}}, \quad (2)$$

where P_{vsat} and P_{atm} are the saturation vapour and atmospheric pressures, respectively, and ϕ is the relative humidity in fraction. The moisture accumulation measurement using the relative humidity sensors has a higher uncertainty (typically ±15%), compared to the measurement using the load sensors (±2%), but provides a useful comparison. The uncertainty in the humidity ratio difference across the test section is the reason for high uncertainty in Δm. For example, a 1.1% uncertainty in the measured RH for a typical 8–10% RH difference between the inlet and outlet, results in an uncertainty in Δm of ±10% to ±14%. The uncertainty in the measurement of moisture accumulation using the relative humidity sensors is typically ±15%.

3.4. Airflow rate and convection transfer coefficient measurements

The airflow rate through the test section is required to calculate the moisture accumulation in the porous bed (Eq. (1)) as well as to quantify the convective heat and mass transfer coefficients above the porous bed. The airflow rate is measured according to ISO 5176-1 [27] with a tapered orifice plate of specific diameter (30 mm and 38 mm during the measurement of spruce plywood and cellulose insulation, respectively) embedded in a circular air duct downstream of the test section (Fig. 1). The pressure difference across the orifice plate (ΔP) is measured with a calibrated pressure differential gauge (uncertainty of ±15 Pa) and the mass flow rate is calculated using Eq. (3) where the air properties are determined upstream of the orifice. The equation for the mass flow is

$$\dot{m}_a = \frac{C_d}{\sqrt{1-\beta^4}} \lambda \frac{\pi}{4} d^2 \sqrt{2\Delta P \rho}, \quad (3)$$

where

$$\beta = \frac{d}{D}, \quad (4)$$

D is the diameter of the supply duct, d is the diameter across the orifice plate, λ [27] is the expansibility factor and C_d is the discharge coefficient. The uncertainty in the mass flow rate is ±6%. The facility is able to generate a range of mass flow rates corresponding to different Re numbers for the airflow in the rectangular duct above the porous bed. The Re is based on the hydraulic diameter (38.4 mm) of the duct and has an uncertainty of ±8%.

A separate test was conducted to determine the convective mass transfer coefficients for these Re numbers [28]. In this test, a tray of water is placed in the TMT facility and air is passed over the free surface of water. As the air with controlled Re number passes over the test section, water evaporates into the air and the mass of water in the tray decreases, which is recorded by the load sensors. The temperature and relative humidity of the air entering and leaving the test section are measured to determine the vapour density of the airflowing above the water. The temperature of the water is also measured to determine the water vapour density at the surface of the water. From the mass readings and vapour densities, the convective mass transfer coefficient is determined. The measured convective mass transfer coefficient is then used to determine the Sherwood number as a function of the Re and Rayleigh numbers. The Rayleigh numbers for the test conditions in this paper (part I and part II [26]) vary over a typical range of 5000–20,000, with higher numbers tending to occur for the turbulent flow tests. These correspond to tests in the lower range of Rayleigh numbers tested in [28] (i.e., 7000 for laminar flow and 20,000 for turbulent flow). Using these constant Rayleigh numbers, the Sherwood number based on the hydraulic diameter of the test section (38.4 mm) can be determined as a function of Re [28]. The resulting correlations for laminar and turbulent flow are, respectively,

$$Sh = \frac{h_m D_h}{D_a} = 0.42\,Re^{0.334}, \quad (5)$$

$$Sh = \frac{h_m D_h}{D_a} = 0.024\,Re^{0.725}. \quad (6)$$

These correlations allow the determination of the convective mass transfer coefficient and convective heat transfer coefficient by applying the analogy between heat and mass transfer (i.e., assuming that the Sherwood number equals the Nusselt number).

4. Preliminary data

In this section, test data obtained for the TMT facility are presented to verify the 1-D temperature and humidity

fields in the porous beds and to quantify the repeatability of the experiments.

4.1. Verification of 1-D heat and moisture transport

Although the porous beds tested in the TMT facility are housed in an impermeable container that is surrounded by thermal insulation, it is important to measure the 3-D humidity and temperature fields in each bed to quantify the extent to which the experiment is 1-D heat and moisture transfer by diffusion only. Each of the materials tested has unique characteristics that could lead to 2-D or 3-D effects becoming important. Cellulose insulation packed at a density of 50 kg/m^3 has reasonably high air permeability [29] and therefore may be susceptible to airflow. To investigate this effect, the temperature difference (ΔT) between each individual thermocouple (T_j) at a certain depth and the average of the five thermocouples (T_{av}) at that depth is presented in Fig. 6a for two different values of Re (1900 and 5000), where

$$\Delta T = T_j - T_{av}. \quad (7)$$

To investigate the effect further, the variation of ΔT at $x = 11$, 22, 33, 44 and 55 mm are shown at different times in Fig. 6b for $Re = 1900$. The initial conditions for this test are 11% RH and 21 °C and the airflow above the insulation is at 70% RH and 21 °C. For $Re = 1900$, the maximum value of ΔT is ±0.15 °C, while the maximum value is ±0.9 °C for $Re = 5000$, suggesting there is a small airflow through the material for $Re = 5000$. This flow of moist air results in 2-D temperature and humidity profiles within the insulation and causes the measured humidity values to exceed those calculated assuming pure diffusion in the insulation as documented in Part II of this paper [26]. The results for other airflow rates used in the cellulose test ($Re = 1600$ and $Re = 2100$) are the same as those for $Re = 1900$. This shows that there is negligible airflow through the material and that the transport process is pure diffusion of heat and water vapour when the airflow above the cellulose is laminar. Since only four humidity sensors are available and the airflow will simultaneously transport heat and water vapour, these tests are not repeated to determine the lateral distribution of humidity. Four thermocouples are also placed on the lexan container: two on the inner and two on the outer side of the container to check for any evidence of heat gain from or heat loss to the surroundings. The results from these thermocouples indicate that there is negligible heat transfer between the cellulose bed and the laboratory air during the experiment.

In case of spruce plywood, no airflow is expected, but the non-homogeneity of the plywood may cause 3-D temperature and humidity fields within the bed. Five relative humidity sensors are placed at a depth of 9 mm to verify the 1-D moisture transfer. The relative humidity readings taken after 2 days of testing are shown in Fig. 6b. The initial conditions for this test are 22% RH and 23 °C and the airflow above the insulation is at 70% RH and 23 °C. The results are shown for two different airflow rates giving $Re = 2000$ and $Re = 4000$ (in the channel above the spruce plywood). For $Re = 2000$, the maximum difference between

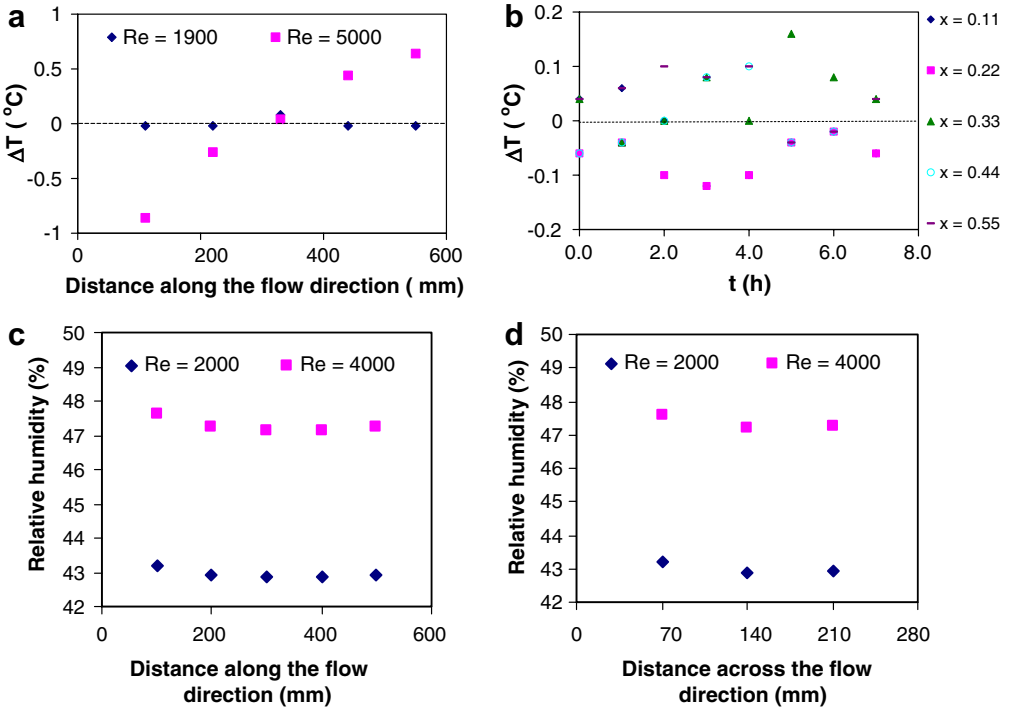

Fig. 6. Difference between individual temperature sensors and the average temperature at a depth of 150 mm (a) after 6 h of testing and (b) at different time intervals for $Re = 1900$ in the cellulose insulation bed. Relative humidity measurements (c) along and (d) across the flow direction at a depth of 9 mm within the spruce plywood after 2 days of testing.

relative humidity readings is 0.3% RH, while the maximum difference is 0.5% RH for $Re = 4000$. These differences are less than the uncertainty in the humidity sensors and thus verify the 1-D moisture transfer created by the impermeable lexan container.

4.2. Repeatability

The repeatability of the experiment is determined using cellulose insulation. The cellulose specimen is initially at equilibrium with air in the laboratory (21 °C and 11% RH) before a laminar airflow ($Re = 1900$) at 21 °C and 70% RH is passed over the insulation. This experiment is performed three times. The differences in the initial conditions in the cellulose insulation from test to test for these repeated tests are within ±0.2% RH and ±0.2 °C. These conditions allows for excellent comparison of the results for the repeated tests and evaluation of the experimental repeatability.

Fig. 7a shows the measured relative humidity for the repeated tests in the cellulose insulation bed for an 8-h period. The measured relative humidities presented in Fig. 7a are the moving averaged results of the measured data (recorded every minute by the data acquisition system) over a 9-min period. These results are at a depth of 60 mm, 120 mm and 180 mm in the cellulose insulation bed. The three tests are labelled test 1, test 2 and test 3 in the order in which they were performed (to distinguish between the tests). The maximum difference in the measured relative humidity between the three tests is 0.8% RH and the average difference at a depth of 60 mm is 0.4% RH. These results show excellent repeatability and the differences in the measured relative humidity are within the uncertainty of the humidity sensors. It should be noted that the fluctuations in the relative humidity of the supply air can also contribute to these small differences in measured relative humidity. Fig. 7b shows the measured temperature in the cellulose insulation for the repeated tests. The results presented are the average of two thermocouple readings for each location. The maximum difference in the measured temperatures between the three tests is 0.3 °C and the average difference at a depth of 60 mm is 0.2 °C. These differences are in the same order as differences in the initial temperatures of the cellulose insulation bed and the fluctuations of the temperature of the supply air, and demonstrate the excellent repeatability of the experiments.

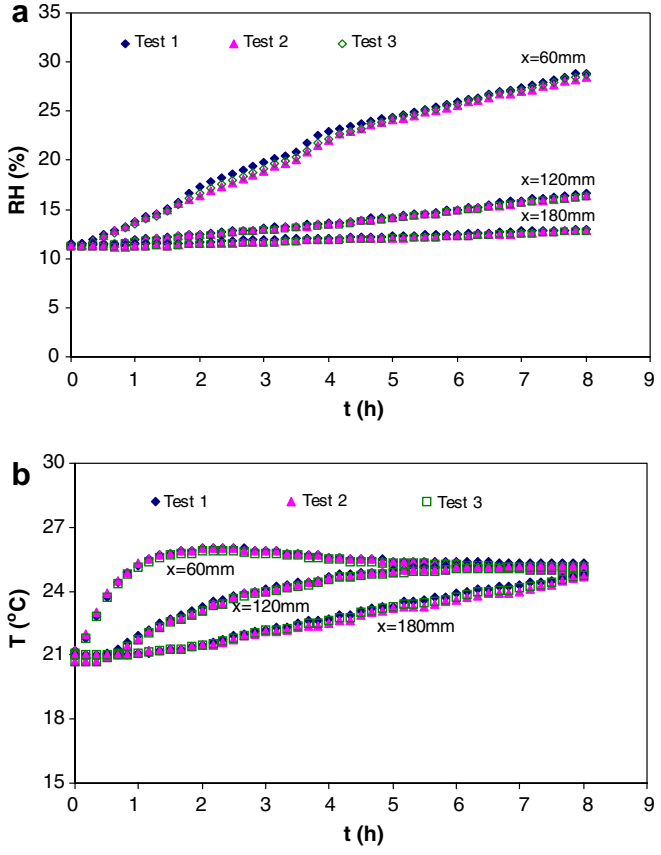

Fig. 7. Measured (a) relative humidity and (b) temperatures in the cellulose insulation bed for the repeatability tests with isothermal test conditions.

5. Material property measurements

Although the measured material properties are not part of the main experiment, these data are required to complete the data set for use when benchmarking models. The measured properties described in this section are the sorption isotherm, effective thermal conductivity and water vapour permeability. Other properties of the spruce plywood at dry condition are dry density (ρ_o) of 445 kg/m^3, porosity (ε_g) of 70%, heat of adsorption (h_{ad}) of 2.5×10^6 J/kg and specific heat capacity ($C_{p_{eff}}$) of 1880 J/(kg K). These properties for dry cellulose insulation are $\rho_o = 50$ kg/m^3, $\varepsilon_g = 0.947$, $h_{ad} = 3.25 \times 10^6$ J/kg and $C_{p_{eff}} = 1400$ J/(kg K).

5.1. Sorption isotherm

The sorption isotherm experiment is performed according to ISO 12571 [30] using salt solutions to generate the relative humidity [31]. The sample specimens are dried using a vented oven at 50 °C (plywood) or a vacuum pump (cellulose) until the change in mass between two successive measurements, with a time interval of at least 24 h, is lower than 0.1%. After drying, the specimens are wrapped in plastic, cooled to room temperature and weighed. The specimens are then placed in the air above saturated salt solutions in 1-L glass jars [32] until equilibrium is reached. The mass is weighed, and the specimens are placed in a jar with a different salt and the process is repeated with increments of about 10% RH up to 97% RH for the adsorption process. For the desorption process, the specimens at 97% RH are placed in jars with a relative humidity of 75% RH until equilibrium is reached. The masses are weighed and then placed in a lower relative humidity with decrements

of about 20% RH up to 11% RH. The moisture content (u) at a given relative humidity is calculated as

$$u = \frac{m - m_o}{m_o}, \tag{8}$$

where m is the final mass of a specimen after equilibrium is attained between the specimen and the air in the jar at a particular relative humidity and m_o is the mass of the dry specimen.

The sorption and desorption curves for spruce plywood are shown in Fig. 8a. The results are averages of the three samples measured. The uncertainty in the mass measurement is ±3 mg and the uncertainty in the moisture content is ±0.0001 kg/kg, which corresponds to an uncertainty in moisture content of ±1% at 11% RH and ±0.1% at 97% RH. The experimental adsorption data are curve fitted with a continuous polynomial relationship between moisture content (u) and relative humidity (ϕ) in fraction. The polynomial equation for the curve fit is given as

$$u = \left(\frac{a + c\phi + e\phi^2}{1 + b\phi + d\phi^2 + f\phi^3}\right) S, \tag{9}$$

where $a = 1.0147\text{E}{-}04$, $b = 0.2339$, $c = 0.06754$, $d = -2.3603$, $e = -0.06574$, $f = 1.1329$. Eq. (9) fits the measured data with $r^2 = 0.999$ when the sensitivity coefficient (S) equals 1. Fig. 8a also shows that Eq. (9) fits the desorption data quite well when $S = 1.1$. Therefore, a ±10% change in the curve fit is representative of the maximum error between the measured data and curve fit, and will be used in the sensitivity studies in part II [26] of this paper.

The sorption isotherm for cellulose insulation is measured in adsorption only on a bed packed to a density of 50 kg/m^3 (Fig. 8a). The curve fit in Fig. 8a is chosen to be consistent with the data in Ref. [29] and yet show good agreement with the experimental data in part II [26] of this paper because there are no measured data between 45% and 75% RH. The experimental adsorption data are curve fitted as

$$\begin{aligned} u &= \frac{a + b\phi + c\phi^2 + d\phi^3 + e\phi^4}{(1.0 + f\phi + g\phi^2 + h\phi^3 + i\phi^4)j} \quad \text{when } \phi \leqslant 0.60, \\ &= k + l\phi(\ln\phi) + m\phi^2 + n/\phi^2 \quad \text{when } \phi > 0.60, \end{aligned} \tag{10}$$

where $a = -0.00007549$, $b = 0.03947$, $c = 0.5952$, $d = -1.168$, $e = 0.5338$, $f = 2.185$, $g = -7.715$, $h = 5.703$, $i = -1.174$, $j = 2.8$, $k = -228.133$, $l = -425.736$, $m = 222.504$ and $n = 6.328$. Eq. (10) fits the measured data with $r^2 = 0.999$.

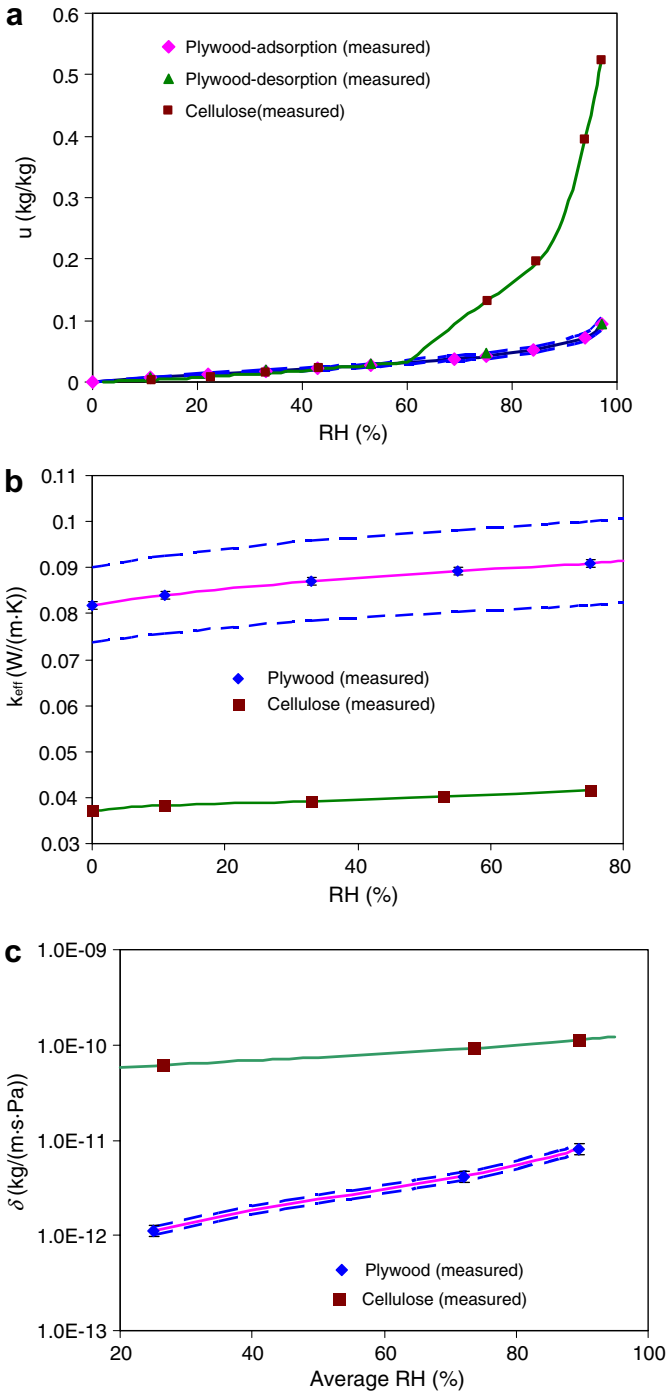

Fig. 8. Measured data and correlations for the (a) sorption isotherm, (b) effective thermal conductivity and (c) water vapor permeability of spruce plywood and cellulose insulation. The dashed lines represent a ±10% change in the correlation.

5.2. Effective thermal conductivity

The effective thermal conductivity of porous materials is measured using a heat flow meter apparatus that measures according to ASTM standard C518 [33]. Prior to testing, the sample is conditioned to different RH values (11%, 33%, 53% and 75% RH) using saturated salt solutions according to ASTM Standard E104 [31] in order to quantify the change in thermal conductivity with equilibrium RH. The effective thermal conductivity is measured three times for each humidity condition using a constant temperature drop of 25 °C across the specimen. The plate temperatures are of 10 °C and 35 °C, giving an average temperature of 22.5 °C. It should be noted that the thermal

conductivity measurements took about 30 min to complete, while it took about 14 days to condition the samples to equilibrium, therefore moisture movement during the thermal conductivity test is expected to be minimal.

For measuring the effective thermal conductivity of spruce plywood, a 9 mm thick piece of spruce plywood with dimensions of 28 mm by 28 mm is used. Fig. 8b presents the average k_{eff} of the three measurements at each RH. Effective thermal conductivity increases with RH as expected. The maximum effective thermal conductivity over the tested range is 0.091 W/(m K), which is 10% higher than the dry value of 0.082 W/(m K). The uncertainty in the measured effective thermal conductivity using the heat flux meter apparatus is ±1% which is about the same size as the data points in Fig. 8b. The experimental data are curved fitted with a continuous relationship that is represented by a polynomial given below:

$$k_{\text{eff}} = (a + b\phi + c\phi^2 + d\phi^3)S, \tag{11}$$

where $a = 0.08185$, $b = 0.02212$, $c = -0.02313$, $d = 0.01291$. Eq. (11) fits the measured data very well when $S = 1$ as shown in Fig. 8b ($r^2 = 0.999$). Fig. 8b also shows a ±10% change in the curve fit for the thermal conductivity, which is representative of the maximum change in k_{eff} from 0% to 75% RH. This ±10% change is not representative of the uncertainty in k_{eff}, but is chosen to be consistent with the ±10% change used for the other properties investigated in the sensitivity studies of the part II [26] of this paper.

To measure the effective thermal conductivity of cellulose insulation, the cellulose fiber insulation is packed to a density of 50 kg/m^3. The experimental data are shown in Fig. 8b and the data are curve fitted with the following polynomial:

$$k_{\text{eff}} = (a + b\phi + c\phi^{1.5} + d\exp(-\phi)), \tag{12}$$

where $a = -0.092482655$, $b = 0.15480621$, $c = -0.066517733$ and $d = 0.1296168$.

5.3. Water vapour permeability

The steady-state water vapour permeability is measured using a modification of the cup method in ASTM Standard E96/E96M-05 (ASTM 2005) [34]. The cups are placed in a small chamber, which is equipped with a small fan (powered by an external motor) to gently mix the air in the chamber with a velocity of 0.06 m/s. Three cup tests are performed at average humidities of 26.5% RH, 73.5% RH and 89% RH created using $CaCl_2$ (0% RH) in the cup and $Mg(NO_3)_2$ (53% RH) in the surrounding air, KNO_3 (94% RH) in the cup and $Mg(NO_3)_2$ (53% RH) in the surrounding air, and KNO_3 (94% RH) in the cup and KCl (84% RH) in the surrounding air, respectively. Prior to testing, the plywood samples are preconditioned at 23 °C and 53% RH in an environmental chamber for 26.5% and 73.5% RH tests and 23 °C and 84% RH for the additional cup test. The cups are weighed periodically to determine the rate of mass transfer through the plywood using a mass balance with an uncertainty of ±0.1 g.

In case of spruce plywood, five circular-shaped samples each 9 mm thick and with an average diameter of 146 mm, are placed in the cups. The edges of the plywood in the cup are sealed with paraffin wax to avoid leakage between the cup and the plywood. The uncertainty in the measured value of the water vapour permeability is ±13%, mainly due to the uncertainty of the variation of the moisture flow through the specimen, which varies slightly from day to day.

The results presented in Fig. 8c show that as the average humidity condition increases, the water vapour permeability increases as expected [29].

The measured data are curve fitted and the relationship is given as

$$\delta = \left(a + \left(\frac{b\phi}{\ln \phi}\right)\right)^{0.5}, \tag{13}$$

where $a = -2.3573\text{E}{-25}$, $b = -8.1601\text{E}{-24}$. Fig. 8c also includes a ±10% change in the curve fit for the vapour permeability, which is representative of the uncertainty in the measured data.

When testing cellulose insulation, the cellulose is packed to a density of 50 kg/m^3 between two wire frames and the same cups are used as with the plywood. The measured data are curve fitted (Fig. 8c) with the following relation:

$$\delta = \left(\frac{1}{a + b\phi}\right), \tag{14}$$

where $a = 1.9435469\text{E}10$ and $b = -1.183156\text{E}8$. Different equations are used to correlate vapour permeability as a function of relative humidity for plywood and cellulose insulation because, as shown in Fig. 8c, the permeability of plywood is more sensitive to changes in relative humidity than cellulose insulation. The correlations are chosen to give the best fit with the measured data.

6. Conclusions

This paper describes an experimental transient moisture transfer (TMT) facility which permits continuous measurements of temperature, relative humidity and moisture accumulation within hygroscopic porous media following step changes in the humidity and/or temperature of the air flowing above the media. The instrumentation, calibration and uncertainties are presented together with preliminary experimental data that demonstrates the repeatability and the physical processes (1-D diffusion heat and moisture transfer) in the experiment for hygroscopic plywood and cellulose insulation. The measured and correlated property data (sorption isotherm, water vapor permeability and effective thermal conductivity) for these materials are also included to fully document the data set in part II of this paper [26] and to allow other researcher to use the data set for model validation. Based on the results in this paper,

the following conclusions can be made about the test facility and experimental data.

- The TMT facility creates 1-D and transient temperature and humidity fields within porous materials and hence the data can be used to benchmark 1-D numerical models of transient diffusion heat and moisture transport in porous materials.
- The total uncertainties (bias plus precision) in the measured temperature, relative humidity and moisture accumulation data obtained from the TMT facility are ± 0.1 °C, $\pm 1\%$ RH and ± 2 g, respectively.
- The TMT facility provides repeatable experimental data. Considering the variation in the boundary conditions for the three repeatability test presented in this paper, the repeatability is smaller than the total uncertainty.

Acknowledgements

The transient moisture transfer facility (TMT) that is described in this paper has been developed with funding from the Canada Foundation for Innovation (CFI), the Saskatchewan Innovation and Science Fund and the University of Saskatchewan. Funding for personnel is from the Natural Science and Engineering Research Council of Canada (NSERC) Discovery and Special Research Opportunity Programs. These financial contributions to the research are greatly appreciated.

References

[1] C.S. Canby, A. Hepbasli, G. Gokcen, Evaluating performance indices of a shopping centre and implementing HVAC control principles to minimize energy usage, Energy Buildings 36 (2004) 587–598.
[2] P.M. Bluyssen, C. Cox, O. Seppänen, E.O. Fernandes, G. Clausen, B. Müller, C.-A. Roulet, Why, when and how do HVAC-systems pollute the indoor environment and what to do about it? The European AIRLESS project, Building Environ. 38 (2003) 209–225.
[3] L. Lu, W. Cai, L. Xie, S. Li, Y.C. Soh, HVAC system optimization—in-buiding section, Energy Buildings 37 (2005) 11–22.
[4] Y. Yao, Y. Jiang, S. Deng, Z. Ma, A study on the performance of the airside heat exchanger under frosting in an air source heat pump water heater/chiller unit, Int. J. Heat Mass Transfer 47 (2004) 3745–3756.
[5] S. Sieniutycz, P. Kuran, Nonlinear models for mechanical energy production in imperfect generators driven by thermal or solar energy, Int. J. Heat Mass Transfer 48 (2005) 719–730.
[6] M.J. Huang, P.C. Eames, B. Norton, Thermal regulation of building-integrated photovoltaics using phase change materials, Int. J. Heat Mass Transfer 47 (2004) 2715–2733.
[7] A.S. Kaiser, M. Lucas, A. Viedma, B. Zamora, Numerical model of evaporative cooling process in a new type of cooling tower, Int. J. Heat Mass Transfer 48 (2005) 986–999.
[8] C.J. Simonson, M. Salonvaara, T. Ojanen, Moderating indoor conditions with hygroscopic building materials and outdoor ventilation, ASHRAE Trans. 110 (2) (2004) 804–819.
[9] C.J. Simonson, M. Salonvaara, T. Ojanen, Heat and mass transfer between indoor air and a permeable and hygroscopic building envelope, Part I – field measurements, J. Therm. Env. Bldg. Sci. 28 (1) (2004) 63–101.
[10] C. Simonson, T. Ojanen, M. Salonvaara, Humidity, comfort and air quality in a bedroom with hygroscopic wooden structures, in: Proceedings (CD) of the Performance of Exterior Envelopes of Whole Buildings, IX International Conference, Clearwater Beach, Florida, 2004, 8 p.
[11] R. Peukhuri, C. Rode, K.K. Hansen, Moisture buffering capacity of different insulation materials, in: Proceedings (CD) of the Performance of Exterior Envelopes of Whole Buildings, IX International Conference, Clearwater Beach, FL, USA, 2004, 14 p.
[12] M. Salonvaara, T. Ojanen, A. Holm, H.M. Kunzel, A.N. Karagiozis, Moisture buffering effects on indoor air quality – experimental and simulation results, in: Proceedings (CD) of the Performance of Exterior Envelopes of Whole Buildings, IX International Conference, Clearwater Beach, Florida, 2004, 11 p.
[13] K. Svennberg, L. Hedegaard, C. Rode, Moisture buffer performance of a fully furnished room, in: Proceedings (CD) of the Performance of Exterior Envelopes of Whole Buildings, IX International Conference, Clearwater Beach, Florida, 2004, 11 p.
[14] L. Fang, G. Clausen, P.O. Fanger, Impact of temperature and humidity on the perception of indoor air quality, Indoor Air 8 (1998) 80–90.
[15] O.F. Osanyintola, C.J. Simonson, Moisture buffering capacity of hygroscopic building materials: experimental facilities and energy impact, Energy Buildings 38 (2006) 1270–1282.
[16] L. Fang, G. Clausen, P.O. Fanger, Impact of temperature and humidity on the perception of indoor air quality during immediate and longer whole-body exposures, Indoor Air 8 (1998) 276–284.
[17] J. Toftum, P.O. Fanger, Air humidity requirements for human comfort, ASHRAE Trans. 105 (2) (1999) 641–647.
[18] O. Adan, H. Brocken, Determination of liquid water transfer properties of porous building material and development of numerical assessment methods, Final Technical Report of the HAMSTAD project, 2003. <http://www.bouw.tno.nl/eng/pdf/Hamstad_finalreport_1.PDF>.
[19] C.-E. Hagentoft, A.S. Kalagasidis, B. Adl-Zarrabi, S. Roels, J. Carmeliet, H. Hens, J. Gruenwald, M. Funk, R. Becker, D. Shamir, O. Adan, H. Brocken, K. Kumaran, R. Djebbar, Assessment method of numerical prediction models for combined heat, air and moisture transfer in building components: benchmarks for one-dimensional cases, J. Therm. Env. Bldg. Sci. 27 (4) (2004) 327–352.
[20] H. Hens, IEA ECBCS Annex 24 final report. Modeling, K.U. Leuven, Belgium, 1996.
[21] P. Warren, Integral building envelope performance assessment, Technical Synthesis Report of IEA ECBCS Annex 32, Integral Building Envelope Performance Assessment, Faber Maunsell Ltd., 2003. <http://www.ecbcs.org/docs/annex_32_tsr_web.pdf>.
[22] H.M. Kunzel, K. Kiessl, Calculation of heat and moisture transfer in exposed building components, Int. J. Heat Mass Transfer 40 (1) (1997) 159–167.
[23] P. Haupl, J. Grunewald, H. Fechner, H. Stopp, Coupled heat air and moisture transfer in building structures, Int. J. Heat Mass Transfer 40 (7) (1997) 1633–1642.
[24] N. Mendes, P.C. Philippi, A method for predicting heat and moisture through multilayered walls based on temperature and moisture content gradients, Int. J. Heat Mass Transfer 48 (2005) 37–51.
[25] P. Mukhopadhyaya, K. Kumaran, F. Tariku, D. van Reenen, Long-term performance: predict the moisture management performance of wall systems as a function of climate, material properties, etc. through mathematical modeling, IRC-RR-132, Ottawa, Canada, 2003. <http://irc.nrc-cnrc.gc.ca/fulltext/rr/rr132>.
[26] Prabal Talukdar, Olalekan F. Osanyintola, Stephen Olutimayin, Carey J. Simonson, An experimental data set for benchmarking 1-D, transient heat and moisture transfer models of porous building materials – Part II: experimental, numerical and analytical data, Int. J. Heat Mass Transfer, in press, doi:10.1016/j.ijheatmasstransfer.2007.03.025.
[27] ISO 5176-1, Measurement of fluid flow by means of pressure differential devices, ISO, Switzerland, 1991.

[28] C.R. Iskra, C.J. Simonson, Convective mass transfer coefficient for a hydrodynamically developed airflow in a short rectangular duct, Int. J. Heat Mass Transfer 50 (2007) 2376–2393.
[29] M.K. Kumaran, A thermal and moisture transport property database for common building and insulating materials, Final Report from ASHRAE Research Project 1018-RP, 2002, 229 p.
[30] ISO 12571, Building materials – determination of hygroscopic sorption curves, ISO, Brussels, 1996.
[31] ASTM E104, Maintaining constant relative humidity by means of aqueous solutions, ASTM, Philadelphia, 1985.
[32] L. Wadso, K. Svennberg, A. Dueck, An experimentally simple method for measuring sorption isotherms, Drying Technol. 22 (10) (2004) 2427–2440.
[33] ASTM C518, Standard test method for steady-state heat flux measurement and thermal transmission properties by means of the heat flow meter apparatus, ASTM Annual book of standards, Philadelphia, 2003, pp. 153–164.
[34] ASTM E96/E96M-05, Standard test method for water vapour transmission of materials, ASTM Annual book of standards, Philadelphia, 2005.